LOSEC: Local Semantic Capture Empowered Large Time Series Model for IoT-Enabled Data Centers

Yu Sun, *Member, IEEE*, Haibo Zhou, *Senior Member, IEEE*, Bo Cheng, *Member, IEEE*, Jinan Li, *Member, IEEE*, Jianzhe Xue, *Member, IEEE*, Tianqi Zhang, *Member, IEEE*, and Yunting Xu, *Member, IEEE*

Abstract—**Deep learning methods for accurately predicting data center status have gained significant attention with the advancement of Internet of Things (IoT) technologies, which make the collection of massive data possible. This capability is crucial for mitigating the exponential growth of energy consumption. However, conventional small models often face data scarcity issues in practical deployment. While large models show promise in addressing this challenge, they encounter obstacles such as multivariate tasks, computational intensity, and ineffective information capture. Moreover, their applications in data centers remain largely unexplored. In this paper, we investigate local semantic capture empowered large model for multivariate time series forecasting in IoT-enabled data centers. We first introduce time series tasks within data centers and propose the Point Lag (Plag)-Llama framework with the Lag-Llama backbone to support zero-shot forecasting and fine-tuning for multivariate point time series forecasting. To address computational intensity and enhance the capabilities of multivariate forecasting, we propose the Local Semantic Capture (LOSEC) for adapter fine-tuning, which captures local semantic information across time and channel dimensions alternately with low-complexity. Specifically, time series are segmented into tokens, and channels are clustered together, forming local semantic information that can be captured more effectively. Extensive experiments demonstrate that Plag-Llama exhibits superior zero-shot capability and that the LOSEC empowered adapter fine-tuning achieves state-of-the-art performance on real-world datasets collected from data centers, with ablation studies further validating the effectiveness of each module within the proposed models.**

Index Terms—**Large model, Internet-of-Things, data center, multivariate time series, parameter-efficient fine-tuning.**

I. Introduction

DATA centers hold a crucial position in global energy consumption and carbon emissions, with their importance projected to escalate exponentially, especially with the widespread adoption of large-scale models like ChatGPT and Llama [2]–[4]. Concurrently, governments and data center operators vigorously enact policies and initiatives targeted at curbing energy consumption [5]. The optimization of cooling systems has garnered significant attention, given their substantial share of energy consumption in data centers. Precise modeling of data centers plays a pivotal role in this context, serving as the key foundation for subsequent optimization algorithms [6]. Recently, the evolution of Internet-of-Things (IoT) techniques has facilitated data-driven modeling [7]–[9], showcasing superiority in providing accurate descriptions of future data center status compared to traditional methods [5], [6], [10]. However, a critical aspect remains unaddressed in these works: multivariate time series forecasting. Despite their successes, these methods encounter challenges related to data scarcity during practical deployment, requiring sufficient data accumulation after all IoT devices are operational, thereby incurring significant time costs.

With the success of large (or foundation) models across various domains [11], recent studies have also explored their significant capabilities in time series forecasting, including Large Language Models (LLMs) based methods [12], [13], foundation models tailored for time series [14], [15]. These models demonstrate superior zero-shot and few-shot abilities, which are anticipated to mitigate the data scarcity challenge, thereby are promising solution to facilitate swift deployment in data centers. However, these methods encounter various challenges to different extents. For example, prompt-based LLMs [12] may struggle with multivariate time series, and the high cost of LLMs presents a barrier to widespread adoption. Furthermore, TimeGPT [14], exclusively available via API, is not suitable for deployment in production environments. Additionally, there has been no prior investigation into the realm of data center applications. There are two approaches to building large models for multivariate time series forecasting in data centers: training from scratch and building upon well-established large models. The massive number of parameters in large models makes it challenging to collect sufficient data for training from scratch in data centers and renders the process computationally expensive [16]. In contrast, building upon existing large models—i.e., fine-tuning—offers a more computationally efficient, less data-intensive approach that fully leverages the capabilities of pre-trained models and yields comparable performance. As a result, the latter approach is preferred. Specifically, we choose to build upon Lag-Llama [15], a State-Of-The-Art (SOTA) time series foundation model designed for univariate probabilistic forecasting. However, it faces several challenges when applied to multivariate time series in data centers. These challenges include: 1) transferring from probabilistic to point forecasting, 2) empowering the multivariate forecasting capabilities of Lag-Llama, and 3) addressing computational intensity and overfitting issues encountered during training.

Part of this work was accepted at the IEEE Global Communications Conference (GLOBECOM) 2024 [1], to be published (*Corresponding author: Haibo Zhou.*).

Y. Sun, H. Zhou, B. Cheng, J. Xue, T. Zhang and Y. Xu are with the School of Electronic Science and Engineering, Nanjing University, Nanjing, China, 210023 (e-mail: yusun@smail.nju.edu.cn, haibozhou@nju.edu.cn, bocheng@smail.nju.edu.cn, jianzhexue@smail.nju.edu.cn, tianqizhang@smail.nju.edu.cn), yuntingxu@smail.nju.edu.cn).

J. Li is with the Guangdong Branch, China Unicom Group Co., Ltd., Guangzhou, China, 510627 (e-mail: eljn@foxmail.com).

These challenges are expected to be addressed through specific fine-tuning methods. However, with the advent and rapid scaling of large models, the computational demands of full fine-tuning have also become prohibitive for most devices and scenarios. Parameter-Efficient Fine-Tuning (PEFT) [17], which modifies only a subset of existing parameters or adds new ones, aims to reduce computational requirements while preserving learned capabilities in large models, enabling them to generalize to new tasks. Nonetheless, existing PEFT methods fail to capture new correlations beyond those encoded in the original models [18], leaving core challenges in Lag-Llama unresolved. Furthermore, many PEFT methods are constrained by simplistic feed-forward [19] or attention-based designs [20] that lack additional information-capturing capabilities, rendering them inadequate for empowering Lag-Llama in multivariate forecasting. Similarly, in multivariate time series tasks, the effectiveness of current channel-dependent attention mechanisms [21], [22] and transformer-based architectures [23] remains debatable, and further investigation is required to address their limitations. Therefore, designing efficient architectures that can effectively capture key and essential information in adapter fine-tuning for multivariate time series, addressing the challenges in Lag-Llama, remains an open problem.

In this paper, we investigate large models empowered by local semantic capture for multivariate time series forecasting in IoT-enabled data centers, addressing data scarcity, capturing semantic information across time and channel dimensions, and achieving SOTA performance. We first introduce the multivariate time series forecasting problem specific to data centers, alongside the large model, Lag-Llama. Subsequently, we propose the point Lag (Plag)-Llama framework, adapted from Lag-Llama, to support zero-shot forecasting and fine-tuning for multivariate point time series forecasting. Furthermore, we propose the **Lo**cal **Se**mantic **C**apture (LOSEC)-empowered adapter fine-tuning technique, which constructs and captures semantic information for both time steps and channels, information that is absent in previous studies but essential for the attention mechanism. This approach enhances the performance of large models for multivariate forecasting while reducing computational intensity. LOSEC alternates between capturing local semantic information across time and channel dimensions with low-complexity: time capture segments the series into tokens for time attention, while channel capture clusters channels for inter-channel attention. Finally, we validate our proposed methods through extensive experiments on real-world datasets, demonstrating their superiority over SOTA approaches. The fundamental contributions are highlighted as follows:

- We construct a multivariate time series forecasting framework for IoT-enabled data centers, employing large models to address data scarcity, facilitate rapid deployment, and achieve SOTA performance. To our knowledge, this is the first effort to apply large models within the data center domain.
- We introduce the Plag-Llama framework, extending Lag-Llama's capabilities from probabilistic univariate to multivariate point time series forecasting, enabling zero-shot ability and full fine-tuning for new tasks. We further propose a novel **Lo**cal **Se**mantic **C**apture (LOSEC) empowered adapter fine-tuning method that reduces computational intensity while achieving SOTA performance.
- We propose LOSEC, a model that alternately constructs and captures local semantic information across time and channel dimensions with low complexity. In this model, time-series data are segmented to form local semantic temporal information, while channels are clustered to generate local semantic channel information. This information is effectively captured through the utilization of multi-head attention mechanisms.

The remainder of this paper is organized as follows. Section III introduces the preliminaries of multivariate time series forecasting in IoT-enabled data centers and describes our adopted backbone large model. The proposed Plag-Llama architecture and the LOSEC empowered adapter fine-tuning method are detailed in Section IV. Experimental results are presented in Section V, followed by the conclusion in Section VII.

II. Related Works

In this section, we review SOTA works relevant to our research, focusing on time series forecasting in data centers, large models for time series forecasting, fine-tuning methods, and mechanisms for capturing correlations in multivariate time series, highlighting their strengths and limitations.

Recently, time series forecasting has become a key foundation for data center optimization [24], [25], with numerous studies exploring this domain. Vu et al. [6] proposed using more appropriate data-driven models by incorporating domain knowledge into their analyses. Specifically, they applied distinct deep learning algorithms tailored to specific module types within a module-wise modeling approach, predicting power, water flow, and water temperature. In contrast, Zhao et al. [5] adopted purely data-driven methods, considering temporal properties within data centers and employing a gated recurrent unit-based approach to leverage historical data for predicting power usage effectiveness. Given the importance of safety-guaranteed optimization in data center operations, Sun et al. [26] leveraged supervised autoencoders to predict cooling capacity and ensure safe operations, achieving accurate predictions with low complexity. To address multiple prediction tasks in data centers, Jiang et al. [10] proposed a model-wise, multi-task transformer-based network to ensure both accuracy and interpretability. However, these works often overlook multivariate and multi-step time series forecasting. Furthermore, traditional small models encounter data scarcity challenges and require substantial time to deploy in real data center scenarios.

With the remarkable success of large models in natural language processing, researchers are increasingly interested in seeing similar capabilities applied to time series forecasting. Recent studies in this area fall into two main categories: transferred large models [12], [13] and foundation models developed specifically for time series [14]. Initially, studies

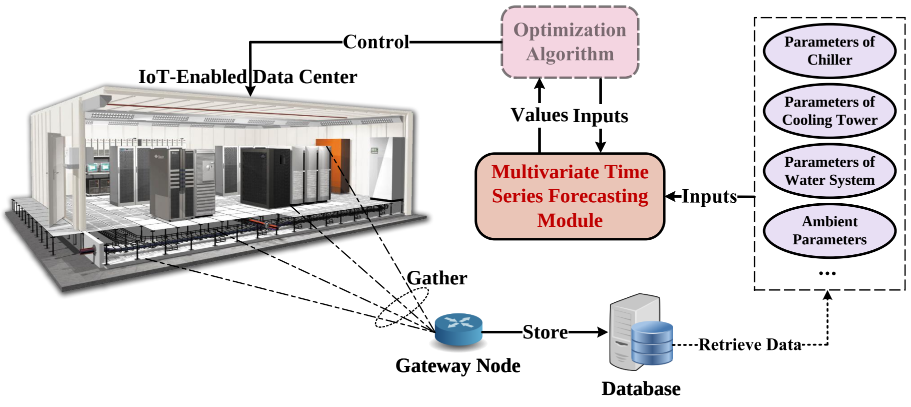

Fig. 1: A framework for multivariate time series forecasting in IoT-enabled data centers.

observed the remarkable capabilities of LLMs, leading to exploration of their application in time series forecasting. Xue et al. [12] directly employed LLMs for forecasting by transforming numerical inputs and outputs into language prompts, demonstrating superior generalization compared to traditional numerical forecasting. To apply LLMs to time series, Jin et al. [13] aligned time series and language modalities by training text prototypes with frozen LLMs, leveraging the internal capabilities of LLMs. Chang et al. [13] pursued a similar approach but proposed a deeper and more flexible fine-tuning method to transfer LLM abilities from natural language to time series, using a two-stage fine-tuning process: supervised fine-tuning for LLMs and task-specific downstream fine-tuning. Moreover, foundation models tailored for time series forecasting have emerged. The first foundation model, TimeGPT [14], based on transformer architecture and trained on 100 billion data points, exhibits high accuracy and strong zero-shot capabilities. In the same vein, Liu et al. [27] developed a GPT-style architecture trained on 1 billion time points, showing promising capabilities across diverse time series applications. Lag-Llama [15], targeting probabilistic univariate time series forecasting, has demonstrated superior performance on various time series datasets. Additional large models for time series forecasting can be found in recent surveys [28]–[30]. However, these foundation models face challenges in multivariate time series forecasting in data centers, such as API-only restrictions that fail to meet privacy requirements in production environments and limitations in capturing multivariate relationships. To the best of our knowledge, no large models have been specifically designed for time series forecasting in data centers.

PEFT methods are promising for adapting large models to downstream tasks and can be categorized into addition-based, selection-based, and reparameterization-based approaches [17]. Specifically, addition-based methods augment original models with extra layers or parameters, fine-tuning only these new parameters. Selection-based methods choose a subset of parameters for fine-tuning, while reparameterization-based methods use low-rank representations to minimize the number of parameters [18]. However, except for adapter-based methods, these approaches struggle to capture new correlations beyond the original models, leaving core challenges in Lag-Llama unsolved. Existing works have explored various adapter architectures as a solution. Houlsby et al. [19] proposed inserting layers serially into original models with bottleneck architectures, yielding compact and extensible models with superior performance. Lei et al. [31] introduced conditional adapters focused on both accuracy and efficiency by skipping heavy computation, achieving faster speeds and improved accuracy. Zhao et al. [20] argue that contexts are more important than the number of parameters. They apply attention layers to adapter fine-tuning to capture conditional position correlations that were missed by previous feed-forward networks, demonstrating superior performance. However, these architectures are limited by simple feed-forward or attention-based designs that lack additional information-capturing capabilities, rendering them insufficient to enhance models like Lag-Llama for multivariate forecasting.

In multivariate time series forecasting, channel-dependent models [32]–[34] intuitively capture correlations between channels to enhance performance. However, recent advances in channel-independent models have demonstrated more superior performance due to separate attention per channel, requiring less data and reducing overfitting [35]. The latest studies [36] suggest that well-designed channel-dependent strategies can effectively capture inter-channel correlations and outperform channel-independent models. Nonetheless, the debate regarding the best method for capturing channel-dependent correlations remains unresolved. These challenges are not limited to channel attention; similar concerns extend to the transformer models themselves. Zeng et al. [23] showed that simple one-layer linear models can outperform some transformer-based SOTA models, raising questions about the true efficacy of transformers for time series forecasting. The discussion surrounding the effectiveness of model architectures in capturing correlations in time series is ongoing. Therefore, designing efficient architectures that can effectively capture channel-dependent and other critical information in time series forecasting remains an open question.

III. Preliminaries

A. Multivariate Time Series Forecasting in IoT-Enabled Data Centers

The framework for multivariate time series forecasting in IoT-enabled data centers is illustrated in Fig. 1. Leveraging advanced IoT technologies, we can monitor the real-time status of data centers by deploying diverse sensors, including those for temperature, humidity, and flow measurement. After deploying all IoT devices, continuous data streams are sensed, collected, and processed by gateway nodes before storage in the database. Over time, as sufficient data accumulates, we retrieve this information-including parameters related to chillers, cooling towers, water systems, ambient conditions, and more-as training data for constructing the multivariate time series forecasting module. Notably, one of our primary motivations is to leverage the few-shot and zero-shot capabilities of foundation models, thus shortening the data accumulation period. Precisely predicting the status of data centers lays the foundation for optimization algorithms[1]. We frame this task as a multivariate time series forecasting problem, capitalizing on the time-dependent intrinsic characteristics and interdependencies among variables.

Let $\mathbf{X} = \{\boldsymbol{x}_1, \boldsymbol{x}_2, \ldots, \boldsymbol{x}_t, \ldots\}$ denote the multivariate time series, where $\boldsymbol{x}_t \in \mathbb{R}^C$ represents the multivariate vector with dimension C (i.e., number of variates or channels) at time t, expressed as $\boldsymbol{x}_t = [x_1, x_2, \ldots, x_C]^T$. The multivariate time series forecasting problem in data centers is defined as follows: Given an L-length context window $\mathbf{X}_{t-L+1:t} \in \mathbb{R}^{C \times L}$, the task aims to accurately predict the future H time steps, i.e., $\mathbf{X}_{t+1:t+H} \in \mathbb{R}^{C \times H}$, by minimizing the following objective:

$$\mathcal{L}\left(\mathbf{X}_{t+1:t+H}, \hat{\mathbf{X}}_{t+1:t+H}\right), \tag{1}$$

where $\mathcal{L}$ represents the loss function, and $\hat{\mathbf{X}}_{t+1:t+H}$ is derived from the multivariate time series forecasting model $\mathcal{M}$:

$$\hat{\mathbf{X}}_{t+1:t+H} = \mathcal{M}\left(\mathbf{X}_{t-L+1:t}\right). \tag{2}$$

B. Lag-Llama

Lag-Llama [15], a foundational model targeting probabilistic univariate time series forecasting, is built upon the decoder-only transformer-based LLaMA architecture, which integrates lagged features. It has demonstrated superior zero-shot ability and state-of-the-art performance across diverse time series datasets. However, it is crucial to recognize that Lag-Llama is designed specifically for univariate forecasting. The superior performance, as emphasized in [15], arises when multivariate time series are processed and forecasted as multiple independent univariate sequences across all benchmark models. Consequently, the adaptation of Lag-Llama to multivariate time series forecasting remains uncertain. Furthermore, in our data center scenarios, our primary requirement is accurate prediction of future status rather than the entire distribution. This necessitates certain modifications to Lag-Llama. Moreover, our experiments with the real-world dataset reveal that Lag-Llama suffers from overfitting. Surprisingly, fine-tuning exacerbates performance rather than improving it. Additionally, the full fine-tuning process for Lag-Llama is computationally intensive and resource-demanding.

[1]The research of optimization algorithms is beyond the scope of this paper.

IV. Model Architecture

A. Plag-Llama: A Multivariate Time Series Point Forecasting Framework

We introduce Plag-Llama, a framework crafted for multivariate time series point forecasting, which extends the capabilities of the pre-trained Lag-Llama. The overall architecture is depicted in Fig. 2. In Lag-Llama, historical inputs $\mathbf{X}_{t-L+1:t} \in \mathbb{R}^{C \times L}$ undergo sequential processing involving a projection layer, N masked transformer decoder layers, and a distribution head, yielding a probabilistic distribution for each time series. To adapt the probabilistic forecasting capability to point forecasting, the pre-trained Lag-Llama, excluding the distribution head, serves as the backbone of Plag-Llama. Furthermore, Plag-Llama integrates supplementary blocks, such as the transfer block and adapter block, incorporates a revised loss function, and employs fine-tuning techniques. The transfer block corresponds to the full fine-tuning method, while the LOSEC adapter block implements the adapter fine-tuning method. As shown in Fig. 2, both methods share a forward pass process, but differ in the backward pass. Specifically, full fine-tuning involves backpropagation through both the pre-trained Lag-Llama model and the transfer block, whereas LOSEC adapter fine-tuning involves backpropagation only through the adapter block and a backward pass through the pre-trained Lag-Llama. This distinction arises from their differing operational mechanisms, which are explained in the following two sections.

B. Full Fine-Tuning

Fine-tuning, as an effective transfer mechanism, has garnered significant attention in the research domain. One of the fundamental methods, the full fine-tuning approach, is also employed in Lag-Llama, wherein all the parameters of the pre-trained model are tuned for new downstream tasks. However, it is important to note that the full fine-tuning strategy used here for Plag-Llama differs from that in Lag-Llama due to the distinct forecasting objectives. Specifically, in Plag-Llama, the distribution head is replaced by a transfer block. Furthermore, the negative log-likelihood loss, typically employed for probabilistic forecasting, is appropriately substituted with the Mean Squared Error (MSE) loss for point forecasting.

Transfer blocks can be implemented in various ways. In this work, we propose an intuitive and zero-shot block that leverages the average operation across feature dimensions:

$$\hat{\mathbf{X}}_{t+1:t+H} = \text{Average}\left(\mathbf{Z}_{t+1:t+H}\right), \tag{3}$$

where $\mathbf{Z}_{t+1:t+H}$ represents the output from the backbone model. The averaging operation is performed along the feature dimension, resulting in $\hat{\mathbf{X}}_{t+1:t+H}$, which directly corresponds to the prediction values. The introduction of the feature-averaging trick is primarily grounded in the consideration of two key factors. Firstly, the foundation model excels in its zero-shot capability, which can be reacquired through this

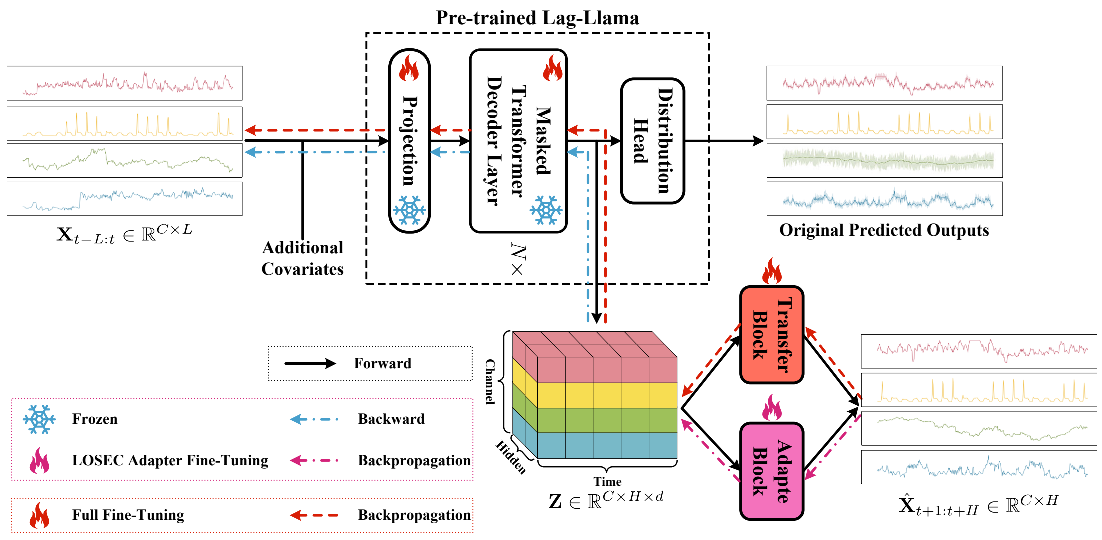

Pre-trained Lag-Llama
Projection
Masked Transformer Decoder Layer
$N\times$
Distribution Head
$\mathbf{X}_{t-L:t} \in \mathbb{R}^{C\times L}$
Additional Covariates
Original Predicted Outputs
Transfer Block
Adapte Block
Channel
Hidden
Time
$\mathbf{Z} \in \mathbb{R}^{C\times H\times d}$
$\hat{\mathbf{X}}_{t+1:t+H} \in \mathbb{R}^{C\times H}$
Forward
Frozen
Backward
LOSEC Adapter Fine-Tuning
Backpropagation
Full Fine-Tuning
Backpropagation

Fig. 2: Plag-Llama: Overview of the architecture.

straightforward method. Secondly, it is essential to acknowledge that a more intricate structure might negatively impact performance during full fine-tuning, given that such a simple trick is also susceptible to overfitting. In the context of Plag-Llama, the update rule for full fine-tuning can be succinctly described as follows:

$$(\boldsymbol{\omega}_{i+1}, \boldsymbol{\theta}_{i+1}) = (\boldsymbol{\omega}_i, \boldsymbol{\theta}_i) - \alpha \nabla \mathcal{L}\left(\boldsymbol{\omega}_i, \boldsymbol{\theta}_i\right), \tag{4}$$

where i denotes the training step, α represents the learning rate, $\boldsymbol{\omega}$ and $\boldsymbol{\theta}$ correspond to the parameters of the backbone and transfer block, respectively, and $\mathcal{L}\left(\boldsymbol{\omega}, \boldsymbol{\theta}\right)$ denotes the loss function. For a comprehensive understanding of the entire full fine-tuning process, encompassing forward, backpropagation, and module update status, please refer to Fig. 2.

C. Local Semantic Capture Empowered Adapter Fine-Tuning

In the full fine-tuning approach, all parameters $\boldsymbol{\omega}$ and $\boldsymbol{\theta}$ must be adjusted for each task, leading to significant computational intensity and resource demands. Despite implementing early stopping and random sampling strategies, full fine-tuning remains prone to overfitting, as demonstrated in Section V. Adapter fine-tuning presents a promising method for capturing new correlations beyond those established by original models, thereby enhancing the capabilities of Lag-Llama in multivariate time series forecasting. However, existing studies [19], [20], [31], [37] fail to adequately capture channel-dependent and other critical information, which would results in a significant degradation of performance. Therefore, in this section, we propose a novel model, LOSEC, aiming capturing local semantic information to compensate drawbacks of base models and achieve SOTA performance.

A primary consideration in adapter fine-tuning is the placement of the inserted module, particularly in light of the challenges posed by Lag-Llama. These challenges include the transition from univariate to multivariate forecasting, as well as from probabilistic to point forecasting, along with issues of computational intensity and overfitting. Fortunately, the adapter inherently mitigates concerns related to point forecasting and overfitting. However, effective multivariate forecasting requires a well-designed strategy for capturing inter-channel dependencies and other essential information, which necessitates significant information flow and may lead to increased computational overhead. Thus, achieving well-balanced trade-offs is crucial for optimal performance. Consequently, we strategically position the adapter module after the masked transformer decoder layer, as illustrated in Fig. 2. This placement ensures that informative channel, time, and feature dimensions are preserved in the outputs.

*1) **Local Semantic Capture**:* To empower Lag-Llama with the ability to perform multivariate forecasting, we seek to understand the correlations between different channels. However, simple attention-based methods struggle to capture this information due to irrelevant and even interfering data among channels [36]. Original attention mechanisms are designed to capture correlations between words in a sentence; however, individual channels in a multivariate time series are more analogous to letters in a sentence, and therefore do not inherently carry semantic meanings. Moreover, this issue extends beyond capturing correlations between channels, affecting the temporal relationships between time steps as well [35]. To address this, we propose the LOSEC model, which constructs and extracts semantic information for both the channel and time dimensions. In this context, certain individuals (channels or time steps) are grouped together to form meaningful semantic units, which we refer to as ”local semantics” due to their localized nature. To efficiently capture local semantic information while maintaining complexity, we first extract local semantics along the time dimension, followed by the channel dimension. This results in two distinct processes: local semantic time capture and local semantic channel capture. This ensures that the attention mechanism can effectively perform its role in capturing these relationships. These captures across the two dimensions are key components of LOSEC. The design philosophy behind these modules is elaborated as

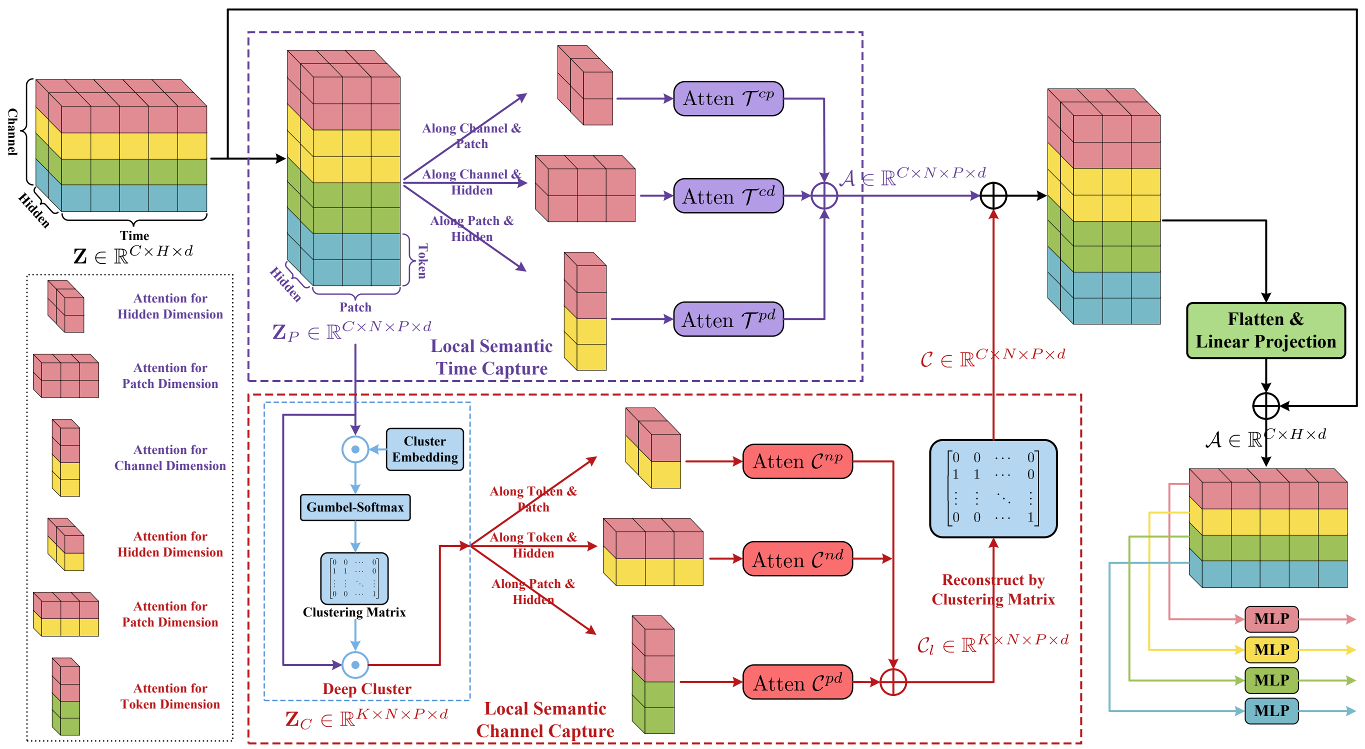
Channel
Hidden
Time
$\mathbf{Z} \in \mathbb{R}^{C\times H\times d}$
Along Channel & Patch
Along Channel & Hidden
Along Patch & Hidden
Token
Hidden
Patch
$\mathbf{Z}_P \in \mathbb{R}^{C\times N\times P\times d}$
Local Semantic Time Capture
Atten $\mathcal{T}^{cp}$
Atten $\mathcal{T}^{cd}$
Atten $\mathcal{T}^{pd}$
$\mathcal{A} \in \mathbb{R}^{C\times N\times P\times d}$
Flatten & Linear Projection
$\mathcal{A} \in \mathbb{R}^{C\times H\times d}$
$\mathcal{C} \in \mathbb{R}^{C\times N\times P\times d}$
Attention for Hidden Dimension
Attention for Patch Dimension
Attention for Channel Dimension
Attention for Hidden Dimension
Attention for Patch Dimension
Attention for Token Dimension
Cluster Embedding
Gumbel-Softmax
Clustering Matrix
Deep Cluster
$\mathbf{Z}_C \in \mathbb{R}^{K\times N\times P\times d}$
Local Semantic Channel Capture
Along Token & Patch
Along Token & Hidden
Along Patch & Hidden
Atten $\mathcal{C}^{np}$
Atten $\mathcal{C}^{nd}$
Atten $\mathcal{C}^{pd}$
Reconstruct by Clustering Matrix
$\mathcal{C}_l \in \mathbb{R}^{K\times N\times P\times d}$
MLP
MLP
MLP
MLP

Fig. 3: Architecture of LOSEC: Capturing local semantic information alternately across time and channel dimensions.

follows:

- **Local Semantic Channel Capture Module:** Analogous to semantics in natural language, we treat channels as letters in a sentence to construct local semantic information by organizing these "letters" (channels) into words. In multivariate time series, some channels exhibit similar variations while others are irrelevant; therefore, an intuitive approach is to assemble similar channels together. Additionally, since channels are unordered, they can be organized arbitrarily. As a result, we cluster channels to construct local semantic channel information within this module. By adopting this local semantic approach, the attention mechanism can operate at the "word" level (i.e., clustered channels), thereby more effectively distinguishing relevant channels from irrelevant ones, reducing noise and interference, and facilitating the identification of key features. This approach also results in a low-complexity design.
- **Local Semantic Time Capture Module:** Similar to the channel dimension design, we treat time steps as letters and organize them into words. Time steps exhibit varying degrees of relevance; unlike channels, time steps are continuous and ordered. Furthermore, neighboring time steps have higher relevance due to temporal dependencies. Therefore, in this module, we cluster time steps while preserving their temporal continuity, specifically through a patching operation on neighboring time steps. This approach enables LOSEC to effectively capture overall trends over time, enhance feature extraction and robustness against noise and interference, and maintain low complexity.

*2) **Overview of LOSEC**:* During the fine-tuning process of the LOSEC adapter for new tasks, we selectively update parameters. Specifically, only the newly introduced parameters $\boldsymbol{\nu}$ within the LOSEC block are adjusted, while the original parameters $\boldsymbol{\omega}$ remain frozen. This adjustment requires a revision of the update rule to:

$$\boldsymbol{\nu}_{i+1} = \boldsymbol{\nu}_i - \alpha \nabla \mathcal{L}'\left(\boldsymbol{\nu}_i\right), \tag{5}$$

where $\mathcal{L}'\left(\boldsymbol{\nu}\right)$ represents the Huber loss, selected for its robustness compared to MSE. The Huber loss is defined as:

$$\text{HuberLoss}\left(y, \hat{y}\right) = \begin{cases} \frac{1}{2}\left(y-\hat{y}\right)^2, & \text{if } |y-\hat{y}| \le \delta, \\ \delta\left(|y-\hat{y}| - \frac{1}{2}\delta\right), & \text{otherwise.} \end{cases} \tag{6}$$

The fine-tuning procedure for the LOSEC is depicted in Fig. 2. In contrast to full backpropagation, which updates all parameters, our proposed approach selectively tunes the adapter block while maintaining the backbone frozen. As a result, backpropagation terminates at the adapter block, and no gradients are propagated to the shallower layers.

The overall architecture of LOSEC is depicted in Fig. 3. The input to LOSEC is the output from the backbone, denoted as $\mathbf{Z} \in \mathbb{R}^{C\times H\times d}$, which contains information regarding time, channels, and hidden dimensions. Initially, the tensor $\mathbf{Z}$ is segmented into patches $\mathbf{Z}_P \in \mathbb{R}^{C\times N\times P\times d}$ and processed by the local semantic time capture module. This module computes attention across the channel & patch, channel & hidden, and patch & hidden dimensions, resulting in the time attention $\mathcal{T} \in \mathbb{R}^{C\times N\times P\times d}$. Next, the patched time series $\mathbf{Z}_P$ is clustered into $\mathbf{Z}_C \in \mathbb{R}^{K\times N\times P\times d}$ and passed through the local semantic channel capture module. This module computes attention along the token & patch, token & hidden, and patch & hidden dimensions, yielding cluster attention $\mathcal{C}_l \in \mathbb{R}^{K \times N \times P \times d}$. Using the clustering matrix, which records channel-cluster mappings, the channel attention is reconstructed, producing $\mathcal{C} \in \mathbb{R}^{C \times N \times P \times d}$. By combining time and channel attention, we obtain $\mathcal{T} + \mathcal{C} \in \mathbb{R}^{C \times N \times P \times d}$. This result is flattened and linearly projected to yield the overall attention $\mathcal{A} \in \mathbb{R}^{C \times H \times d}$. The final predicted output, $\hat{\mathbf{X}}_{t+1:t+H}$, is obtained by adding a residual connection and passing through the corresponding MLP layer. Detailed descriptions of the local semantic time capture and local semantic channel capture modules are provided in the following sections.

*3) **Local Semantic Time Capture**:* To capture local semantic information over the time dimension, we first partition the matrix $\mathbf{Z}$ into semantic tokens $\mathbf{Z}_P \in \mathbb{R}^{C \times N \times P \times d}$, where $N = \lfloor \frac{H-P}{S} + 1 \rfloor$. We apply multi-head self-attention over time to identify correlations among these semantic tokens. Since $\mathbf{Z}_P$ is high-dimensional, flattening $N \times P \times d$ and treating it as the hidden dimension would result in high computational complexity, requiring $\mathcal{O}(C^2 NPd)$. Instead, we propose capturing local semantic information alternately across specific dimensions, applying time attention to channel-patch, channel-hidden, and patch-hidden combinations, respectively, as shown in Fig. 3. Specifically, $\mathbf{Z}_P$ is sliced alternately along these dimensions, with attention operations defined accordingly:

For time attention across the hidden dimension, we slice $\mathbf{Z}_P$ along channel and patch dimensions, forming sets $\left\{\mathbf{Z}_P^{cp} \in \mathbb{R}^{N \times d}, c = 1, 2, \ldots, C, p = 1, 2, \ldots, P\right\}$. We then derive query, key, and value matrices based on $\mathbf{Z}_P^{cp}$:

$$\mathbf{Q}^{cp} = F_q^{cp}\left(\mathbf{Z}_P^{cp}\right), \tag{7a}$$

$$\mathbf{K}^{cp} = F_k^{cp}\left(\mathbf{Z}_P^{cp}\right), \tag{7b}$$

$$\mathbf{V}^{cp} = F_v^{cp}\left(\mathbf{Z}_P^{cp}\right), \tag{7c}$$

where $\mathbf{Q}^{cp}, \mathbf{K}^{cp}, \mathbf{V}^{cp} \in \mathbb{R}^{N \times d}$, and $F_q^{cp}, F_k^{cp}, F_v^{cp}$ are linear transformation layers. Multi-head attention is also adopted to better capture their correlations:

$$\mathcal{T}_i^{cp} = \text{softmax}\left(\frac{1}{\sqrt{d}} \mathbf{Q}_i^{cp} (\mathbf{K}_i^{cp})^T\right) \mathbf{V}_i^{cp},\ i = 1, 2, \ldots, h^{cp}, \tag{8}$$

where $\mathcal{T}_i^{cp} \in \mathbb{R}^{N \times d_h}$ represents attention for head i, and $\mathbf{Q}_i^{cp}, \mathbf{K}_i^{cp}, \mathbf{V}_i^{cp} \in \mathbb{R}^{N \times d_h}$ are query, key, and value matrices for head i derived from $\mathbf{Q}^{cp}, \mathbf{K}^{cp}, \mathbf{V}^{cp}$. The number of heads and head dimension are denoted by h^{cp} and d_h, respectively.

Similarly, based on sliced sets $\left\{\mathbf{Z}_P^{cd} \in \mathbb{R}^{N \times P}, c = 1, 2, \ldots, C, d = 1, 2, \ldots, d\right\}$, we derive time attention across the patch dimension:

$$\mathbf{Q}^{cd} = F_q^{cd}\left(\mathbf{Z}_P^{cd}\right), \tag{9a}$$

$$\mathbf{K}^{cd} = F_k^{cd}\left(\mathbf{Z}_P^{cd}\right), \tag{9b}$$

$$\mathbf{V}^{cd} = F_v^{cd}\left(\mathbf{Z}_P^{cd}\right), \tag{9c}$$

$$\mathcal{T}_i^{cd} = \text{softmax}\left(\frac{1}{\sqrt{P}} \mathbf{Q}_i^{cd} \left(\mathbf{K}_i^{cd}\right)^T\right) \mathbf{V}_i^{cd},\ i = 1, 2, \ldots, h^{cd}, \tag{10}$$

where $\mathcal{T}_i^{cd} \in \mathbb{R}^{N \times P_h}$, $\mathbf{Q}_i^{cd}, \mathbf{K}_i^{cd}, \mathbf{V}_i^{cd} \in \mathbb{R}^{N \times P_h}$.

By slicing and transposing matrices, we obtain sets $\left\{\mathbf{Z}_P^{pd} \in \mathbb{R}^{N \times C}, p = 1, 2, \ldots, P, d = 1, 2, \ldots, d\right\}$, enabling time attention across the channel dimension:

$$\mathbf{Q}^{pd} = F_q^{cd}\left(\mathbf{Z}_P^{pd}\right), \tag{11a}$$

$$\mathbf{K}^{pd} = F_k^{pd}\left(\mathbf{Z}_P^{pd}\right), \tag{11b}$$

$$\mathbf{V}^{pd} = F_v^{pd}\left(\mathbf{Z}_P^{pd}\right), \tag{11c}$$

$$\mathcal{T}_i^{pd} = \text{softmax}\left(\frac{1}{\sqrt{C}} \mathbf{Q}_i^{pd} \left(\mathbf{K}_i^{pd}\right)^T\right) \mathbf{V}_i^{pd},\ i = 1, 2, \ldots, h^{pd}, \tag{12}$$

where $\mathcal{T}_i^{pd} \in \mathbb{R}^{N \times C_h}$, $\mathbf{Q}_i^{pd}, \mathbf{K}_i^{pd}, \mathbf{V}_i^{pd} \in \mathbb{R}^{N \times C_h}$.

The overall time attention is then computed as follows:

$$\mathcal{T}_{c,n,p,d} = \mathcal{T}_{c,p}^{cp} + \mathcal{T}_{c,d}^{cd} + \mathcal{T}_{p,d}^{pd}, \tag{13}$$

where $\mathcal{T}_{c,n,p,d}$ is the (c, n, p, d) element in the time attention matrix $\mathcal{T} \in \mathbb{R}^{C \times N \times P \times D}$, $\mathcal{T}_{c,p}^{cp}$ is the (c, p) element in $\mathcal{T}^{cp}$, $\mathcal{T}_{c,d}^{cd}$ is the (c, d) element in $\mathcal{T}^{cd}$, and $\mathcal{T}_{p,d}^{pd}$ is the (p, d) element in $\mathcal{T}^{pd}$. The matrices $\mathcal{T}^{cp}$, $\mathcal{T}^{cd}$, and $\mathcal{T}^{pd}$ are the concatenations of their respective attention heads:

$$\mathcal{T}^{cp} = \left[\mathcal{T}_1^{cp}, \mathcal{T}_2^{cp}, \ldots, \mathcal{T}_{h^{cp}}^{cp}\right], \tag{14a}$$

$$\mathcal{T}^{cd} = \left[\mathcal{T}_1^{cd}, \mathcal{T}_2^{cd}, \ldots, \mathcal{T}_{h^{cd}}^{cd}\right], \tag{14b}$$

$$\mathcal{T}^{pd} = \left[\mathcal{T}_1^{pd}, \mathcal{T}_2^{pd}, \ldots, \mathcal{T}_{h^{pd}}^{pd}\right]. \tag{14c}$$

*4) **Local Semantic Channel Capture**:* To capture local semantic information over channel dimensions, we cluster channels into clusters, which also reduces attention complexity by focusing on clusters rather than individual channels. We cluster $\mathbf{Z}_P$ along the channel dimension into K clusters, denoted as $\mathbf{Z}_C \in \mathbb{R}^{K \times N \times P \times d}$. There are various methods to cluster C channels into K clusters; here, we consider a deep learning-based approach that is simple and compatible with our overall framework. We aim to assign a probability $p_{c,k}$ for channel c and cluster k, represented as the normalized inner product of two vectors. One of these vectors is the input $\mathbf{Z}_p$, and we also need to define an initialized K cluster embedding $\mathbf{C} \in \mathbb{R}^{K \times d}$. Consequently, the probability matrix $\mathbf{P} \in \mathbb{R}^{C \times N \times P \times K}$ can be computed as follows:

$$\mathbf{P}_{c,n,p,k} = \sum_d \mathbf{Z}_{P(c,n,p,d)} \cdot \mathbf{C}_{k,d}, \tag{15}$$

where $\mathbf{P}_{c,n,p,k}$ is the (c, n, p, k) element of $\mathbf{P}$, $\mathbf{Z}_{P(c,n,p,d)}$ is the (c, n, p, d) element of $\mathbf{Z}_P$, $\mathbf{C}_{k,d}$ is the (k, d) element of $\mathbf{C}$. We expect the clustering assignment matrix to be a one-hot matrix, that is, $\mathbf{A} \in \mathbb{R}^{C \times N \times P \times K}$, $\mathbf{A}_{c,n,p,k} \sim \text{Bernoulli}(p_{c,k})$. Although the softmax operation can ensure that the probability distribution satisfies $\sum_k \mathbf{P}_{c,n,p,k} = 1$, the $\arg\max\ \mathbf{P}_{c,n,p,k}$ operation is not differentiable and does not preserve the probability distrubtion, rendering backpropagation infeasible and clustering less useful. Therefore, we utilize a reparameterization trick along with the softmax operation, specifically Gumbel-Softmax [38], to make the clustering assignment matrix differentiable and approximate the Bernoulli distribution, which is defined as follows:

$$\mathbf{A}_{c,n,p,i} = \frac{\exp\left(\left(\log(\mathbf{P}_{c,n,p,i}) + g_i\right)/\tau\right)}{\sum_{j=1}^{k} \exp\left(\left(\log(\mathbf{P}_{c,n,p,j}) + g_j\right)/\tau\right)}, \quad i = 1, 2, \ldots, k, \tag{16}$$

where g_i are i.i.d. samples drawn from the Gumbel distribution, and τ is the temperature parameter. Subsequently, the clustered $\mathbf{Z}_C$ can be obtained as:

$$\mathbf{Z}_{C(k,n,p,d)} = \sum_{c} \mathbf{Z}_{P(c,n,p,d)} \cdot \mathbf{A}_{c,n,p,k}. \tag{17}$$

Based on the clustered $\mathbf{Z}_C$, we can derive the channel attention in a manner similar to obtaining token attention as follows:

$$\mathbf{Q}^{np} = F_q^{np}\left(\mathbf{Z}_C^{np}\right), \tag{18a}$$
$$\mathbf{K}^{np} = F_k^{np}\left(\mathbf{Z}_C^{np}\right), \tag{18b}$$
$$\mathbf{V}^{np} = F_v^{np}\left(\mathbf{Z}_C^{np}\right), \tag{18c}$$

$$\mathcal{C}_i^{np} = \operatorname{softmax}\left(\frac{1}{\sqrt{d}} \mathbf{Q}_i^{np} (\mathbf{K}_i^{np})^T\right) \mathbf{V}_i^{np}, \ i = 1, 2, \ldots, h^{np}, \tag{19}$$

where $\mathcal{C}_i^{np}$ denotes channel attention regarding the hidden dimension, $\left\{\mathbf{Z}_C^{np} \in \mathbb{R}^{K \times d}, n = 1, 2, \ldots, N, p = 1, 2, \ldots, P\right\}$, $\mathcal{C}_i^{np} \in \mathbb{R}^{K \times d_h}$, $\mathbf{Q}_i^{np}, \mathbf{K}_i^{np}, \mathbf{V}_i^{np} \in \mathbb{R}^{K \times d_h}$.

$$\mathbf{Q}^{nd} = F_q^{nd}\left(\mathbf{Z}_C^{nd}\right), \tag{20a}$$
$$\mathbf{K}^{nd} = F_k^{nd}\left(\mathbf{Z}_C^{nd}\right), \tag{20b}$$
$$\mathbf{V}^{nd} = F_v^{nd}\left(\mathbf{Z}_C^{nd}\right), \tag{20c}$$

$$\mathcal{C}_i^{nd} = \operatorname{softmax}\left(\frac{1}{\sqrt{P}} \mathbf{Q}_i^{nd} \left(\mathbf{K}_i^{nd}\right)^T\right) \mathbf{V}_i^{nd}, \ i = 1, 2, \ldots, h^{nd}, \tag{21}$$

where $\mathcal{C}_i^{nd}$ represents channel attention concerning the patch dimension, $\left\{\mathbf{Z}_C^{nd} \in \mathbb{R}^{K \times P}, n = 1, 2, \ldots, N, d = 1, 2, \ldots, d\right\}$, $\mathcal{C}_i^{nd} \in \mathbb{R}^{K \times P_h}$, $\mathbf{Q}_i^{nd}, \mathbf{K}_i^{nd}, \mathbf{V}_i^{nd} \in \mathbb{R}^{K \times P_h}$.

$$\mathbf{Q}^{c,pd} = F_q^{c,pd}\left(\mathbf{Z}_C^{c,pd}\right), \tag{22}$$

$$\mathbf{K}^{c,pd} = F_k^{c,pd}\left(\mathbf{Z}_C^{c,pd}\right), \tag{23}$$

$$\mathbf{V}^{c,pd} = F_v^{c,pd}\left(\mathbf{Z}_C^{c,pd}\right), \tag{24}$$

$$\mathcal{C}_i^{pd} = \operatorname{softmax}\left(\frac{1}{\sqrt{P}} \mathbf{Q}_i^{c,pd} \left(\mathbf{K}_i^{c,pd}\right)^T\right) \mathbf{V}_i^{c,pd}, \quad i = 1, 2, \ldots, h^{c,pd}, \tag{25}$$

where $\mathcal{C}_i^{pd}$ denotes channel attention with respect to the token dimension, $\left\{\mathbf{Z}_C^{c,pd} \in \mathbb{R}^{K \times N}, p = 1, 2, \ldots, P, d = 1, 2, \ldots, d\right\}$, $\mathcal{C}_i^{c,pd} \in \mathbb{R}^{K \times N_h}$, $\mathbf{Q}_i^{c,pd}, \mathbf{K}_i^{c,pd}, \mathbf{V}_i^{c,pd} \in \mathbb{R}^{K \times N_h}$.

Therefore, the overall channel attention is computed as follows:

$$\mathcal{C}_{c,n,p,d} = \mathcal{C}_{n,p}^{np} + \mathcal{C}_{n,d}^{nd} + \mathcal{C}_{p,d}^{pd}, \tag{26}$$

where $\mathcal{C}^{cp}, \mathcal{C}^{cd}, \mathcal{C}^{pd}$ are the concatenations of their respective heads.

D. Streamlined Complexity: The Efficient Design of LOSEC

LOSEC is a low-complexity model featuring three key design strategies to achieve reduced computational complexity:

- **Formation of local semantic information across time and channel dimensions:** The local semantic information block forms semantic structures while lowering complexity. For the time dimension, segment H time series into N tokens, reducing complexity from $\mathcal{O}\left(H^2\right)$ to $\mathcal{O}\left(H^2/S^2\right)$, with N on the order of $\mathcal{O}\left(H/S\right)$. For the channel dimension, cluster C channels into K clusters, reducing complexity from $\mathcal{O}\left(C^2\right)$ to $\mathcal{O}\left(K^2\right)$.
- **Alternating capture over time and channel dimensions:** Instead of requiring global attention with a complexity of $\mathcal{O}\left(C^2H^2\right)$, alternating between dimensions reduces the complexity to $\mathcal{O}\left(\max\left(C^2, H^2\right)\right)$.
- **Dimension-specific attention mechanisms:** When capturing attention across time or channel dimensions, the remaining dimensions are not flattened but treated alternately as hidden dimensions, reducing complexity from $\mathcal{O}\left(C^2NPd\right)$ to $\mathcal{O}\left(C^2 \cdot \max\left(N, P, d\right)\right)$ for channel attention and from $\mathcal{O}\left(N^2CPd\right)$ to $\mathcal{O}\left(N^2 \cdot \max\left(C, P, d\right)\right)$ for time attention.

These three designs work together to streamline complexity in LOSEC. Specifically, the overall complexity is derived as follows: We employ a multi-head self-attention mechanism to capture local semantic information within the proposed LOSEC model. Consequently, the complexity is directly determined by the self-attention operation, which is expressed as $\mathcal{O}(n^2d)$, where n represents the sequence length, and d denotes the model's dimensionality [39]. For local semantic time capture, the time attention $\mathcal{T}^{cp}$, applied across hidden dimensions of length N and dimension d, incurs a computational cost of $\mathcal{O}\left(N^2d\right)$ per channel and patch. This results in a total complexity of $\mathcal{O}\left(CPN^2d\right)$. Similarly, the complexities of $\mathcal{T}^{cd}$ and $\mathcal{T}^{pd}$ are $\mathcal{O}\left(CdN^2P\right)$ and $\mathcal{O}\left(PdN^2C\right)$, respectively. Hence, the overall complexity for local semantic time capture is $\mathcal{O}\left(CN^2Pd\right)$. For local semantic channel capture, the channel attention $\mathcal{C}^{np}$, applied across hidden dimensions of length K and dimension d, incurs a computational cost of $\mathcal{O}\left(K^2d\right)$ per patch, yielding a total complexity of $\mathcal{O}\left(NPK^2d\right)$. Similarly, the complexities of $\mathcal{C}^{nd}$ and $\mathcal{C}^{pd}$ are $\mathcal{O}\left(NdK^2P\right)$ and $\mathcal{O}\left(PdK^2N\right)$, respectively. Therefore, the overall complexity for local semantic channel capture is $\mathcal{O}\left(K^2NPd\right)$. Combining these two modules, the total computational complexity of the LOSEC model is $\mathcal{O}\left(NPd \cdot \max\left(CN, K^2\right)\right)$.

V. Experiments

A. Experimental Settings

Dataset. We utilize data collected from a real data center [25], obtained through various IoT devices with sampling intervals of one or two minutes. The data is processed using linear interpolation, Z-score normalization, and the box-and-whisker plot method to identify outliers. The resulting multivariate time series consists of one-minute intervals across 130 dimensions, totaling 274,662 samples.

TABLE I: Multivariate time series forecasting performance: The context length is set to 8, and the prediction length is set to 4 (best results in **bold**, second best in underlined, and third best in dotted underline).

MODEL	MAE	MSE	SMAPE	MASE	ARk
SUPERVISED					
Autoformer	0.139	0.180	26.244	0.184	8.75
Crossformer	0.137	0.190	23.863	0.181	8.75
DLinear	0.135	0.179	24.786	0.178	6.50
FEDformer	0.141	0.182	26.858	0.186	9.75
Informer	0.128	0.179	22.939	0.169	3.50
iTransformer	0.135	0.245	19.451	0.178	6.25
LightTS	0.168	0.204	34.194	0.222	12.50
NS-Transformer	0.130	0.182	22.971	0.171	5.75
PatchTST	0.136	0.249	**19.424**	0.179	7.25
TimesNet	0.130	0.187	22.580	0.171	5.00
Transformer	0.353	0.397	67.239	0.466	14.00
ZERO-SHOT					
Plag-Llama	0.127	0.194	20.579	0.180	5.75
FINE-TUNING					
Plag-Llama (Full)	0.153	**0.176**	28.643	0.201	9.25
Plag-Llama (LOSEC Adapter)	**0.123**	0.177	21.980	**0.162**	**2.00**

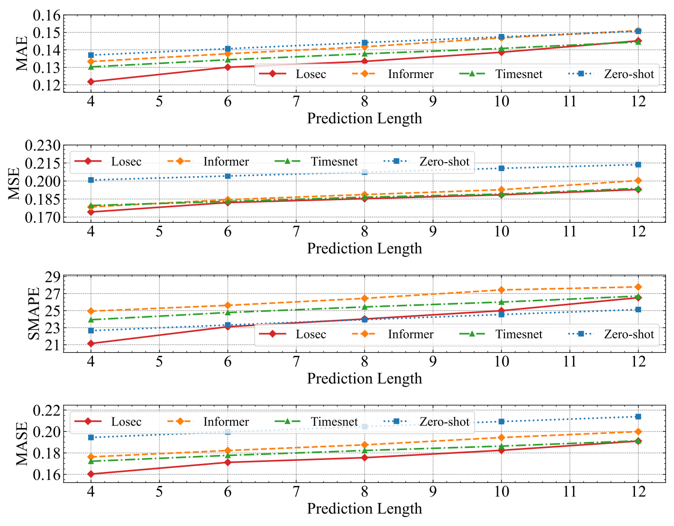

Fig. 4: Multivariate time series performance comparison versus different prediction lengths.

Baselines. We establish the following recent state-of-the-art methods as baselines: Autoformer [40], Crossformer [41], DLinear [23], FEDformer [21], Informer [42], iTransformer [32], LightTS [43], Non-stationary (NS)-Transformer [44], PatchTST [35], TimesNet [33], and Transformer [25]. The default parameters are configured as follows: the number of epochs is set to 50; the Huber loss hyperparameter δ is set to 0.005; and the learning rate is 3e-4. The patch size is 2, with a stride of 1. The number of clusters K is set to 64, the context length is set to 8, and the prediction length is set to 4. By default, the number of attention heads is 8, although it may vary based on the head dimension (using the greatest common divisor). The hidden layer sizes of the multi-layer perceptron (MLP) are set to 256, 128, 64, and 32, respectively. The Adam optimizer is employed, while other parameters adhere to their originally recommended values.

Metrics. We employ commonly used metrics in time series forecasting, including Mean Absolute Error (MAE), Mean Squared Error (MSE), Symmetric Mean Absolute Percentage Error (SMAPE), and Mean Absolute Scaled Error (MASE). Additionally, we calculate the average rank (ARk) across these metrics.

B. Multivariate Time Series Forecasting Performance

We compare our proposed methods with SOTA models in the data center multivariate time series forecasting task. The results for three categories: supervised, zero-shot, and fine-tuning models are summarized in Table I. Leveraging the powerful forecasting capabilities of Lag-Llama and the proposed transfer block, Plag-Llama demonstrates strong zero-shot performance, achieving the second-best MAE and third-best SMAPE, along with an average rank of 5.75. Although it falls short of the best performance, it still ranks third among the supervised SOTA models. This superior zero-shot performance indicates that the Plag-Llama framework is a promising solution to address data scarcity challenges and expedite deployment within data centers. It is important to note that the original Lag-Llama aims to align the overall distribution with the ground truth; however, the simple average layer effectively transfers these probabilistic capabilities to point forecasting. This is attributed to the symmetric Student's t-distribution adopted in Lag-Llama, where learning optimal mean values is beneficial for probabilistic forecasting. However, full fine-tuning significantly undermines the performance of Plag-Llama due to overfitting, resulting in an average rank of 9.25, which is even worse than its zero-shot performance. Empowered by the proposed local semantic information capture framework, the LOSEC adapter consistently demonstrates superior performance compared to other SOTA models, exhibiting an average improvement of 3.34% over the second-best model.

Based on the above results, we further explore the performance of the models versus different prediction lengths. We select the two best supervised models, zero-shot Plag-Llama, and the LOSEC adapter for this comparison. As the prediction length increases, models face greater challenges, as illustrated in Fig. 4. LOSEC consistently outperforms other models, except for the SMAPE metric, where it slightly underperforms compared to zero-shot Plag-Llama when the prediction length exceeds 10. These results demonstrate that LOSEC can effectively capture local semantic information across both channel and time dimensions, showcasing SOTA performance in multivariate time series forecasting tasks.

C. Few-Shot Ability

To assess the few-shot capabilities of our proposed models in comparison to SOTA methods, we train on the last 20%, 40%, 60%, and 80% of the dataset using both supervised learning from scratch and fine-tuning techniques. The results, presented in Table II, show that LOSEC consistently outperforms SOTA models across various few-shot ratios, achieving results comparable to the top-performing supervised models, specifically PatchTST and TimesNet. However, PatchTST and TimesNet exhibit instability, with performance occasionally declining as more historical data is introduced, suggesting

TABLE II: Comparison of few-shot abilities: The context length is set to 8, and the prediction length is set to 4 (best results in **bold**, second best in underlined, and third best in dotted underline).

DATA %	MODEL	MAE	MSE	SMAPE	MASE	ARk
20 %	Autoformer	0.141	0.181	26.745	0.186	7.50
	Crossformer	0.143	0.189	23.991	0.188	8.00
	DLinear	0.135	0.177	25.151	0.179	6.00
	FEDformer	0.145	0.186	27.870	0.191	9.50
	Informer	0.134	0.182	24.174	0.176	6.25
	iTransformer	0.133	0.207	21.653	0.175	5.50
	LightTS	0.373	0.369	70.688	0.492	12.00
	NS-Transformer	0.132	0.181	23.919	0.174	4.50
	PatchTST	**0.130**	0.208	**20.527**	**0.172**	3.50
	TimesNet	0.131	0.179	23.847	0.173	**3.00**
	Transformer	0.484	0.557	92.126	0.639	13.00
	Plag-Llama (Full)	0.156	**0.166**	31.457	0.205	8.50
	Plag-Llama (LOSEC Adapter)	0.132	0.179	24.885	0.173	3.75
40 %	Autoformer	0.141	0.184	26.375	0.186	8.50
	Crossformer	0.156	0.190	28.696	0.206	10.25
	DLinear	0.137	0.172	26.154	0.180	5.75
	FEDformer	0.142	0.184	27.218	0.188	9.00
	Informer	0.130	0.180	23.389	0.172	4.25
	iTransformer	0.132	0.223	19.925	0.174	5.75
	LightTS	0.170	0.208	31.831	0.224	11.50
	NS-Transformer	0.130	0.181	23.153	0.172	4.00
	PatchTST	0.132	0.227	**19.729**	0.175	6.25
	TimesNet	0.130	0.181	23.012	0.171	3.00
	Transformer	0.407	0.445	80.859	0.537	13.00
	Plag-Llama (Full)	0.140	**0.168**	29.339	0.184	7.00
	Plag-Llama (LOSEC Adapter)	**0.128**	0.178	23.576	**0.168**	**2.75**
60 %	Autoformer	0.140	0.181	26.287	0.184	7.00
	Crossformer	0.161	0.193	28.054	0.212	9.50
	DLinear	0.141	**0.172**	28.392	0.186	6.75
	FEDformer	0.142	0.183	26.933	0.187	8.50
	Informer	0.130	0.179	23.411	0.172	3.25
	iTransformer	0.132	0.227	19.713	0.174	5.75
	LightTS	0.172	0.212	32.919	0.227	11.25
	NS-Transformer	0.130	0.181	23.274	0.172	4.50
	PatchTST	0.133	0.235	**19.559**	0.176	6.25
	TimesNet	0.129	0.180	23.026	0.170	**2.50**
	Transformer	0.367	0.405	71.127	0.485	13.00
	Plag-Llama (Full)	0.172	0.180	35.518	0.226	9.75
	Plag-Llama (LOSEC Adapter)	**0.129**	0.180	23.835	**0.169**	3.00
80 %	Autoformer	0.139	0.180	26.245	0.184	6.00
	Crossformer	0.210	0.209	37.375	0.277	10.75
	DLinear	0.218	0.198	49.875	0.288	11.00
	FEDformer	0.142	0.183	27.261	0.188	7.75
	Informer	0.130	0.180	23.278	0.171	3.50
	iTransformer	0.134	0.236	19.541	0.176	5.75
	LightTS	0.153	0.205	27.751	0.202	9.50
	NS-Transformer	0.130	0.182	22.981	0.172	4.50
	PatchTST	0.134	0.239	**19.520**	0.177	6.25
	TimesNet	0.130	0.183	22.876	0.171	4.00
	Transformer	0.387	0.423	77.318	0.511	13.00
	Plag-Llama (Full)	0.148	0.180	29.369	0.195	7.50
	Plag-Llama (LOSEC Adapter)	**0.127**	**0.178**	22.695	**0.167**	**1.50**

sensitivity to noisy data. Additionally, our proposed LOSEC model employs an adapter fine-tuning approach that leverages its generalization ability, adjusting only a subset of parameters for new tasks rather than training entirely from scratch. Although full fine-tuning of Plag-Llama achieves slightly better performance with less data, its overall results are limited by overfitting. Reducing the data size somewhat alleviates this issue, but the underlying problem persists.

Overall, these results demonstrate that Plag-Llama performs strongly in multivariate time series forecasting, especially in zero-shot and few-shot scenarios. Our analysis further highlights that while full fine-tuning of Plag-Llama can lead to overfitting, LOSEC effectively mitigates this issue by leveraging a more effective adapter fine-tuning approach. By adjusting only a subset of parameters, LOSEC achieves better generalization without the pitfalls of overfitting, yielding more stable results across varied data contexts. Taken together, these experiments emphasize LOSEC's effectiveness from multiple perspectives, showcasing its advantages over SOTAs and traditional full fine-tuning methods.

D. Visualization of Local Semantic Information Caputure

*1) **LOSEC over Channel**:* Fig. 5a presents a t-SNE visualization of time series data along the channel dimension, where each point represents a channel within a sample, and each color denotes a distinct channel type. For simplicity, we display only the first 10 channels. It is evident that channels 2, 3, 5, 6, 7, 8, and 9 are closely positioned in the t-SNE space, suggesting they may form a cohesive cluster. In contrast, channels 0, 1, and 4 are more distinct from this cluster and from each other. The similarity matrices in Fig. 5b and 5c confirm these observations, highlighting strong correlations between certain channels. In Fig. 5b, dark regions or bands appear in the similarity map, indicating clusters of channels with consistent similarity patterns. These dark regions correspond to groups of channels with higher mutual correlations, while channels outside these areas or in lighter regions exhibit lower correlation, implying more diverse or independent feature sets. Fig. 5c provides more detailed correlations among the first 10 channels, where channels 2, 3, 5, 6, 7, 8, and 9 show high similarity scores, while channels 0, 1, and 4 are notably less similar to both each other and the other channels. This observation aligns with conclusions from Fig. 5a. The visualizations above reveal strong correlations within specific channel clusters, while distinct features separate different clusters. These findings highlight the necessity of capturing inter-channel correlations without interference from unrelated channels, emphasizing the importance of capturing local semantic information across channels. Notably, local semantic information within the channel dimension is visually manifested as dark regions in the similarity map, representing clusters of related channels.

To validate that LOSEC effectively captures local semantic information in the channel dimension, we also visualize LOSEC's attention maps over this dimension. Fig. 6a shows attention maps between clusters, while Fig. 6b reconstructs these maps through a cluster-channel mapping matrix. Fig. 6c shows the future time-step similarity map across channels. The reconstructed channel attention map closely aligns with this similarity map, confirming that LOSEC effectively captures channel correlations through clustering.

*2) **LOSEC over Time**:* Fig. 7a shows the similarity map between context time steps. We observe a strong correlation between adjacent time steps, with nearby steps showing particularly high correlations. This suggests that consecutive time steps are inherently related, reflecting a natural continuity over

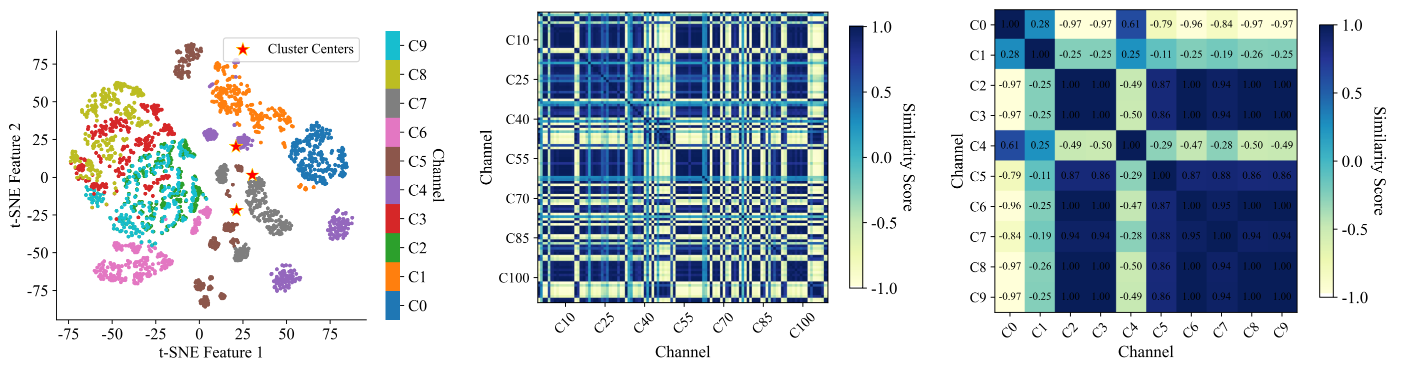

(a) (b) (c)

Fig. 5: Visualization of input channel correlations. (a) t-SNE clustering visualization for the first 10 channels; (b) similarity matrix visualization for all channels; (c) similarity matrix visualization for the first 10 channels.

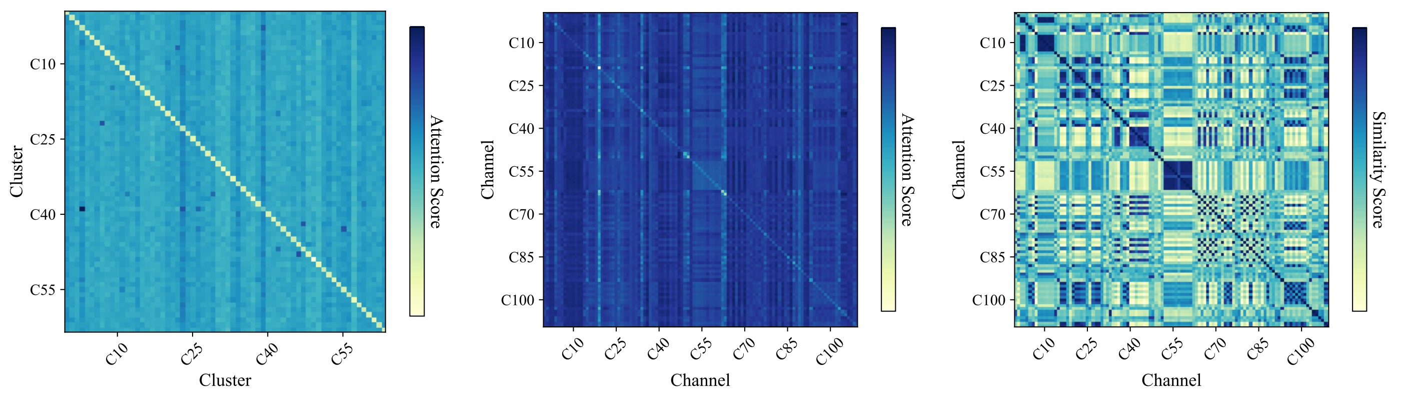

(a) (b) (c)

Fig. 6: Visualization of LOSEC's attention map across the channel dimension. (a) cluster attention map visualization; (b) channel attention map visualization; (c) similarity matrix visualization for future time-step.

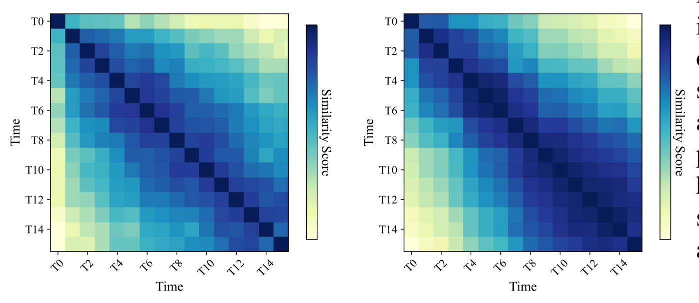

(a) (b)

Fig. 7: Visualization of attention map of LOSEC over channel dimension. (a) visualization of cluster attention map; (b) visualization of channel attention map; (c) visualization of similarity matrix for **future correlations**.

time, where each time step has contextual dependencies on its neighbors. The adopted patching strategy in LOSEC groups consecutive time steps together, enabling the model to fully exploit adjacent correlations, i.e., local semantic information. Patching facilitates the extraction of local semantic features from multiple time steps. This patch-level information is essential for improving the model's ability to extract correlated features (such as time continuity and dependencies over short intervals), aggregate useful information, and reduce noise, offering advantages not present in step-level attention. Fig. 7b shows the similarity map between future time steps after apply LOSE module without patching. Although there is no patching here, it shows more distinct adjacent time steps high correlations than cotnext time steps. It further validate such correlations are common, also patching mechanism is advantages in our experiments.

VI. Ablation Studies

In this section, to further validate the effectiveness of the proposed LOSEC model and clarify the roles of its individual modules, we conduct ablation studies on context length, attention across channel and time dimensions, cluster ratio, and patch size.

A. *Influence of Context Length*

We further investigate model performance across different context lengths, comparing the top two supervised models, zero-shot Plag-Llama, and the LOSEC adapter. As shown in Fig. 8, LOSEC consistently outperforms other models on most

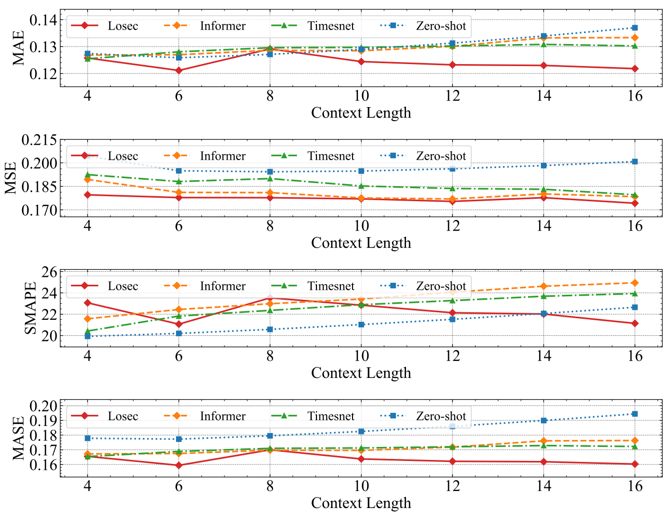

Fig. 8: Multivariate time series performance comparison versus different context lengths.

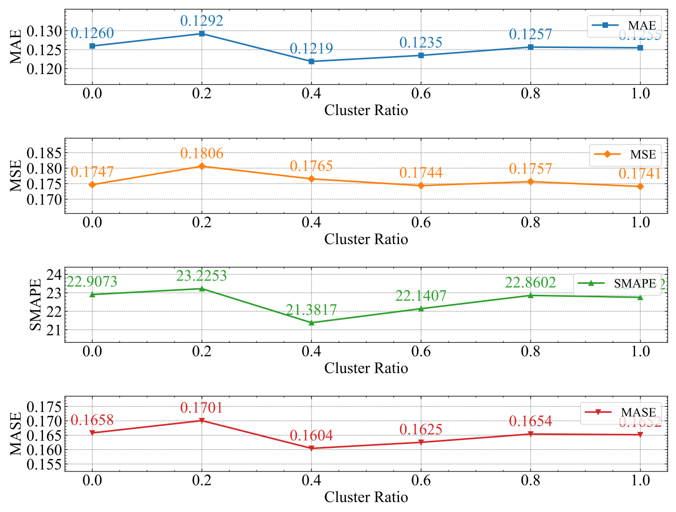

Fig. 9: Ablation study on channel clustering: The context length is set to 8, and the prediction length is set to 4.

TABLE III: Ablation study on attention across channel and time dimensions in the LOSEC adapter (Channel+Time refers to the original LOSEC, Time refers to attention only over time, Channel refers to attention only over the channel, and None refers to the absence of attention).

MODEL	MAE	MSE	SMAPE	MASE	ARk
LOSEC					
Channel+Time	**0.123**	0.177	**21.980**	**0.162**	**1.25**
Time	0.127	**0.176**	23.858	0.168	2.25
Channel	0.437	0.427	92.403	0.576	5.00
None	0.130	0.178	23.468	0.171	3.50
SOTA					
Informer	0.128	0.179	22.939	0.169	3.00

metrics, except for SMAPE, where it achieves comparable performance. Furthermore, as context length increases, the performance of zero-shot Plag-Llama, Informer, and TimesNet deteriorates significantly, while LOSEC maintains stable and superior performance. A longer context length provides more valuable historical information, but it also introduces additional noise and interference. Consequently, these models struggle with longer contexts, whereas LOSEC demonstrates robustness and an enhanced ability to capture relevant information amid interference.

B. Influence of Attention across Channel & Time Dimension

To investigate the effects of attention mechanisms across channel and time dimensions, we sequentially remove time and channel attention to create three configurations: time-only, channel-only, and no-attention. We also use the best-performing supervised model, Informer, as the baseline SOTA. When channel attention is removed, LOSEC shows an 8.54% decrease in SMAPE and a 3.73% average decrease, yet it still outperforms the SOTA model, highlighting the importance of capturing inter-channel correlations. Separately, removing time attention results in a significant degradation in LOSEC's performance, reducing it to below the configuration without any attention. This result confirms the essential role of time attention. Although channel attention captures inter-channel correlations, it may miss channel-specific information when considered alone, leading to diminished performance. This information loss has minimal impact on LOSEC's performance, as time attention preserves complete information with low complexity, allowing LOSEC to sustain strong performance with reduced complexity. With both attention mechanisms removed, LOSEC's performance, while still comparable to SOTA, decreases substantially compared to the original LOSEC (by 4.65% on average). This result confirms LOSEC's robust time series forecasting capability and underscores the necessity and effectiveness of capturing local semantic information across both channel and time dimensions.

C. Influence of Channel Cluster

As shown in Fig. 9, we vary the cluster ratio from 0.0 to 1.0 with intervals of 0.2, where 0.0 represents all channels fused into a single channel, and 1.0 indicates that each channel remains individual without clustering. Our findings reveal that a fully unclustered approach (1.0) is not optimal, highlighting interference and noise among channels. Purely global attention cannot capture these inter-channel correlations effectively, which helps explain why channel-dependent models may underperform compared to channel-independent ones. Therefore, LOSEC's approach of clustering channels to capture local semantic information is essential, as it reduces interference and noise among channels. Subsequent experimental results further underscore the LOSEC model's effectiveness and superiority over SOTA methods. Clustering all channels into one (0.0) is also suboptimal, as it discards inter-channel information, retaining only averaged features. Nevertheless, even at a 0.0 clustering ratio, LOSEC performs well, surpassing SOTA models. These results indicate that averaging channels is not necessarily a poor choice. Additionally, some channel information is preserved through time attention, which helps retain performance. Therefore, LOSEC achieves SOTA performance even with a single-channel cluster, maintaining remarkably low complexity. Furthermore, in our experiments, LOSEC achieves the best performance when the cluster ratio is within

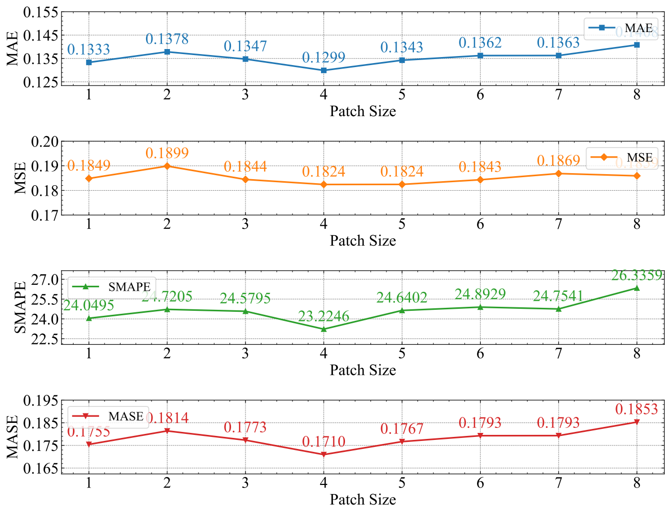

Fig. 10: Ablation study on time patching: The context length is set to 16, and the prediction length is set to 8.

$[0.4, 0.6]$, though this may vary with different datasets and tasks. This parameter can be selected to balance performance and complexity depending on the specific task.

D. *Influence of Time Patching*

We also investigate the impact of time patching, as shown in Fig. 10, where the patch size ranges from 1 to 8, with a patch size of 1 indicating no patching. A larger patch size captures more global information and reduces complexity but may result in the loss of local details. Our results indicate that the optimal patch size is approximately 4 in this experiment, which outperforms no patching by an average of 2.47%. The best patch size varies depending on the dataset and task, and its selection should balance complexity and accuracy. Based on these results, we conclude that LOSEC's approach to capturing local information over time through patching is both crucial and instrumental in enhancing model performance.

VII. Conclusion

In this paper, we have investigated large models empowered by local semantic capture for multivariate time series forecasting in IoT-enabled data centers, an approach that addresses data scarcity, facilitates rapid deployment, and achieves superior performance. We have adapted Lag-Llama for multivariate point time series forecasting, incorporating zero-shot, few-shot and fine-tuning capabilities, by proposing the framework Plag-Llama. Additionally, we have designed a novel Local Semantic Capture model for adapter fine-tuning, which captures local semantic information across patched time and clustered channels. Extensive experiments have demonstrated the superior performance of the proposed models, while ablation studies have validated the rationale and effectiveness of our design philosophy, particularly the construction and capture of semantic information. In the future, we will apply our models to multivariate time series forecasting in various domains to further validate their superiority and contribute to achievements in other areas.

References

[1] Y. Sun, B. Cheng, J. Li, G. Jiang, T. Zhang, and H. Zhou, "Plag-llama for IoT-enabled data centers: A multivariate time series forecasting approach," in *GLOBECOM 2024 - 2024 IEEE Global Communications Conference*.

[2] G. Sun, W. Xie, D. Niyato, H. Du, J. Kang, J. Wu, S. Sun, and P. Zhang, "Generative AI for advanced UAV networking," Apr. 2024.

[3] J. Wang, H. Du, D. Niyato, J. Kang, S. Cui, X. Shen, and P. Zhang, "Generative AI for integrated sensing and communication: Insights from the physical layer perspective," *IEEE Wireless Communications*, vol. 31, no. 5, pp. 246–255, Oct. 2024.

[4] C. Zhang, G. Sun, J. Li, Q. Wu, J. Wang, D. Niyato, and Y. Liu, "Multi-objective aerial collaborative secure communication optimization via generative diffusion model-enabled deep reinforcement learning," *IEEE Transactions on Mobile Computing*, pp. 1–18, 2024.

[5] P. Zhao, L. Yang, Z. Kang, and J. Lin, "On Predicting the PUE with Gated Recurrent Unit in Data Centers," in *2019 IEEE 5th International Conference on Computer and Communications (ICCC)*, Dec. 2019, pp. 1664–1670.

[6] H. D. Vu, K. S. Chai, B. Keating, N. Tursynbek, B. Xu, K. Yang, X. Yang, and Z. Zhang, "Data Driven Chiller Plant Energy Optimization with Domain Knowledge," in *Proceedings of the 2017 ACM on Conference on Information and Knowledge Management*, ser. CIKM '17. New York, NY, USA: Association for Computing Machinery, Nov. 2017, pp. 1309–1317.

[7] Y. Xu, H. Zhou, T. Ma, J. Zhao, B. Qian, and X. Shen, "Leveraging multiagent learning for automated vehicles scheduling at nonsignalized intersections," *IEEE Internet of Things Journal*, vol. 8, no. 14, pp. 11 427–11 439, Jul. 2021.

[8] Y. Xu, B. Qian, K. Yu, T. Ma, L. Zhao, and H. Zhou, "Federated learning over fully-decoupled RAN architecture for two-tier computing acceleration," *IEEE Journal on Selected Areas in Communications*, vol. 41, no. 3, pp. 789–801, Mar. 2023.

[9] J. Xue, K. Yu, T. Zhang, H. Zhou, L. Zhao, and X. Shen, "Cooperative Deep Reinforcement Learning Enabled Power Allocation for Packet Duplication URLLC in Multi-Connectivity Vehicular Networks," *IEEE Transactions on Mobile Computing*, vol. 23, no. 8, pp. 8143–8157, Aug. 2024.

[10] G. Jiang, Y. Sun, B. Cheng, Y. Wang, and H. Zhou, "Leveraging multi-task learning for energy consumption prediction in IoT-based data center," in *2023 IEEE 23rd International Conference on Communication Technology (ICCT)*, Oct. 2023, pp. 943–948.

[11] J. Wang, H. Du, Y. Liu, G. Sun, D. Niyato, S. Mao, D. I. Kim, and X. Shen, "Generative AI based secure wireless sensing for ISAC networks," Aug. 2024.

[12] H. Xue and F. D. Salim, "PromptCast: A new prompt-based learning paradigm for time series forecasting," *IEEE Transactions on Knowledge and Data Engineering*, pp. 1–14, 2023.

[13] M. Jin, S. Wang, L. Ma, Z. Chu, J. Y. Zhang, X. Shi, P.-Y. Chen, Y. Liang, Y.-F. Li, S. Pan, and Q. Wen, "Time-LLM: Time series forecasting by reprogramming large language models," *arXiv preprint arXiv:2310.01728*, Oct. 2023.

[14] A. Garza and M. Mergenthaler-Canseco, "TimeGPT-1," *arXiv preprint arXiv:2310.03589*, Oct. 2023.

[15] K. Rasul, A. Ashok, A. R. Williams, H. Ghonia, R. Bhagwatkar, A. Khorasani, M. J. D. Bayazi, G. Adamopoulos, R. Riachi, N. Hassen, M. Biloš, S. Garg, A. Schneider, N. Chapados, A. Drouin, V. Zantedeschi, Y. Nevmyvaka, and I. Rish, "Lag-llama: Towards foundation models for probabilistic time series forecasting," *arXiv preprint arXiv:2310.08278*, Feb. 2024.

[16] W. X. Zhao, K. Zhou, J. Li, T. Tang, X. Wang, Y. Hou, Y. Min, B. Zhang, J. Zhang, Z. Dong, Y. Du, C. Yang, Y. Chen, Z. Chen, J. Jiang, R. Ren, Y. Li, X. Tang, Z. Liu, P. Liu, J.-Y. Nie, and J.-R. Wen, "A survey of large language models," Oct. 2024.

[17] V. Lialin, V. Deshpande, and A. Rumshisky, "Scaling down to scale up: A guide to parameter-efficient fine-tuning," *arXiv preprint arXiv:2303.15647*, Mar. 2023.

[18] Z. Han, C. Gao, J. Liu, J. Zhang, and S. Q. Zhang, "Parameter-efficient fine-tuning for large models: A comprehensive survey," Apr. 2024.

[19] N. Houlsby, A. Giurgiu, S. Jastrzebski, B. Morrone, Q. D. Laroussilhe, A. Gesmundo, M. Attariyan, and S. Gelly, "Parameter-efficient transfer learning for NLP," in *Proceedings of the 36th International Conference on Machine Learning*. PMLR, May 2019, pp. 2790–2799.

[20] H. Zhao, H. Tan, and H. Mei, "Tiny-attention adapter: Contexts are more important than the number of parameters," Oct. 2022.

[21] T. Zhou, Z. Ma, Q. Wen, X. Wang, L. Sun, and R. Jin, "FEDformer: Frequency enhanced decomposed transformer for long-term series forecasting," in *Proceedings of the 39th International Conference on Machine Learning*. PMLR, Jun. 2022, pp. 27 268–27 286.

[22] A. Dosovitskiy, L. Beyer, A. Kolesnikov, D. Weissenborn, X. Zhai, T. Unterthiner, M. Dehghani, M. Minderer, G. Heigold, S. Gelly, J. Uszkoreit, and N. Houlsby, "An image is worth 16x16 words: Transformers for image recognition at scale," Jun. 2021.

[23] A. Zeng, M. Chen, L. Zhang, and Q. Xu, "Are transformers effective for time series forecasting?" *Proceedings of the AAAI Conference on Artificial Intelligence*, vol. 37, no. 9, pp. 11 121–11 128, Jun. 2023.

[24] Y. Wang, Y. Sun, B. Cheng, G. Jiang, and H. Zhou, "DQN-based chiller energy consumption optimization in IoT-enabled data center," in *2023 IEEE 23rd International Conference on Communication Technology (ICCT)*, Oct. 2023, pp. 985–990.

[25] Y. Sun, Y. Wang, G. Jiang, B. Cheng, and H. Zhou, "Deep learning-based power usage effectiveness optimization for IoT-enabled data center," *Peer-to-Peer Networking and Applications*, Mar. 2024.

[26] Y. Sun, B. Cheng, G. Jiang, Y. Wang, and H. Zhou, "Cooling capacity prediction for safety-guaranteed optimization in IoT-enabled data center," in *2023 IEEE 23rd International Conference on Communication Technology (ICCT)*, Oct. 2023, pp. 920–925.

[27] Y. Liu, H. Zhang, C. Li, X. Huang, J. Wang, and M. Long, "Timer: Generative pre-trained transformers are large time series models," in *Forty-First International Conference on Machine Learning*, Jun. 2024.

[28] M. Jin, Q. Wen, Y. Liang, C. Zhang, S. Xue, X. Wang, J. Zhang, Y. Wang, H. Chen, X. Li, S. Pan, V. S. Tseng, Y. Zheng, L. Chen, and H. Xiong, "Large models for time series and spatio-temporal data: A survey and outlook," Oct. 2023.

[29] Y. Jiang, Z. Pan, X. Zhang, S. Garg, A. Schneider, Y. Nevmyvaka, and D. Song, "Empowering time series analysis with large language models: A survey," Feb. 2024.

[30] M. Jin, Y. Zhang, W. Chen, K. Zhang, Y. Liang, B. Yang, J. Wang, S. Pan, and Q. Wen, "Position paper: What can large language models tell us about time series analysis," Feb. 2024.

[31] T. Lei, J. Bai, S. Brahma, J. Ainslie, K. Lee, Y. Zhou, N. Du, V. Zhao, Y. Wu, B. Li, Y. Zhang, and M.-W. Chang, "Conditional adapters: Parameter-efficient transfer learning with fast inference," *Advances in Neural Information Processing Systems*, vol. 36, pp. 8152–8172, Dec. 2023.

[32] Y. Liu, T. Hu, H. Zhang, H. Wu, S. Wang, L. Ma, and M. Long, "Itransformer: Inverted transformers are effective for time series forecasting," *arXiv preprint arXiv:2310.06625*, 2023.

[33] H. Wu, T. Hu, Y. Liu, H. Zhou, J. Wang, and M. Long, "TimesNet: Temporal 2D-variation modeling for general time series analysis," in *The Eleventh International Conference on Learning Representations*, Sep. 2022.

[34] L. Zhao and Y. Shen, "Rethinking channel dependence for multivariate time series forecasting: Learning from leading indicators," Feb. 2024.

[35] Y. Nie, N. H. Nguyen, P. Sinthong, and J. Kalagnanam, "A time series is worth 64 words: Long-term forecasting with transformers," in *The Eleventh International Conference on Learning Representations*, Sep. 2022.

[36] J. Chen, J. E. Lenssen, A. Feng, W. Hu, M. Fey, L. Tassiulas, J. Leskovec, and R. Ying, "From similarity to superiority: Channel clustering for time series forecasting," Mar. 2024.

[37] K. Li, W. Gu, M. Xue, J. Xiao, D. Shi, and X. Wei, "Atten-adapter: A unified attention-based adapter for efficient tuning," in *2023 IEEE International Conference on Image Processing (ICIP)*, Oct. 2023, pp. 1265–1269.

[38] S. Chen, L. Li, G. Wang, M. Pang, and C. Shen, "Federated Learning with Heterogeneous Quantization Bit Allocation and Aggregation for Internet of Things," *IEEE Internet of Things Journal*, pp. 1–1, 2023.

[39] A. Vaswani, N. Shazeer, N. Parmar, J. Uszkoreit, L. Jones, A. N. Gomez, Ł. Kaiser, and I. Polosukhin, "Attention is All you Need," in *Advances in Neural Information Processing Systems*, vol. 30. Curran Associates, Inc., 2017.

[40] H. Wu, J. Xu, J. Wang, and M. Long, "Autoformer: Decomposition Transformers with Auto-Correlation for Long-Term Series Forecasting," in *Advances in Neural Information Processing Systems*, vol. 34. Curran Associates, Inc., 2021, pp. 22 419–22 430.

[41] Y. Zhang and J. Yan, "Crossformer: Transformer utilizing cross-dimension dependency for multivariate time series forecasting," in *The Eleventh International Conference on Learning Representations*, Sep. 2022.

[42] H. Zhou, S. Zhang, J. Peng, S. Zhang, J. Li, H. Xiong, and W. Zhang, "Informer: Beyond efficient transformer for long sequence time-series forecasting," *Proceedings of the AAAI Conference on Artificial Intelligence*, vol. 35, no. 12, pp. 11 106–11 115, May 2021.

[43] D. Campos, M. Zhang, B. Yang, T. Kieu, C. Guo, and C. S. Jensen, "LightTS: Lightweight time series classification with adaptive ensemble distillation," *Proceedings of the ACM on Management of Data*, vol. 1, no. 2, pp. 171:1–171:27, Jun. 2023.

[44] Y. Liu, H. Wu, J. Wang, and M. Long, "Non-stationary transformers: Exploring the stationarity in time series forecasting," *Advances in Neural Information Processing Systems*, vol. 35, pp. 9881–9893, Dec. 2022.